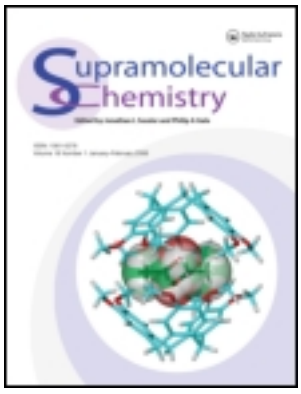

Supramolecular Chemistry
Publication details, including instructions for authors and subscription information:
http://www.tandfonline.com/loi/gsch20

Enantioselective recognition of dicarboxylic acid guests based on an allosteric effect of a chiral double-decker porphyrin which changes the stoichiometry upon the guest binding

Tomohiro Ikeda [a b], Kazuki Sada [b], Seiji Shinkai [b c] & Masayuki Takeuchi [a]

[a] Macromolecules Group, National Institute for Materials Science, Organic Nanomaterials Centre, Tsukuba, 305-0047, Japan

[b] Department of Chemistry and Biochemistry, Graduate School of Engineering, Kyushu University, Fukuoka, 819-0395, Japan

[c] Institute of Systems, Information Technologies and Nanotechnologies, Fukuoka, 814-0012, Japan

Available online: 31 Aug 2010

To cite this article: Tomohiro Ikeda, Kazuki Sada, Seiji Shinkai & Masayuki Takeuchi (2011): Enantioselective recognition of dicarboxylic acid guests based on an allosteric effect of a chiral double-decker porphyrin which changes the stoichiometry upon the guest binding, Supramolecular Chemistry, 23:01-02, 59-64

To link to this article: http://dx.doi.org/10.1080/10610278.2010.510191

Supramolecular Chemistry
Vol. 23, Nos. 1–2, January–February 2011, 59–64

Enantioselective recognition of dicarboxylic acid guests based on an allosteric effect of a chiral double-decker porphyrin which changes the stoichiometry upon the guest binding

Tomohiro Ikeda[a,b], Kazuki Sada[b], Seiji Shinkai[b,c] and Masayuki Takeuchi[a]*

[a]*Macromolecules Group, National Institute for Materials Science, Organic Nanomaterials Centre, Tsukuba 305-0047, Japan;* [b]*Department of Chemistry and Biochemistry, Graduate School of Engineering, Kyushu University, Fukuoka 819-0395, Japan;* [c]*Institute of Systems, Information Technologies and Nanotechnologies, Fukuoka 814-0012, Japan*

(*Received 3 June 2010; final version received 12 July 2010*)

A double-decker porphyrin $\mathbf{1_R}$ bearing one chiral substituent per porphyrin ring was synthesised. The host $\mathbf{1_R}$ showed highly cooperative binding towards chiral guest $\mathbf{2_R}$ with stoichiometry of the complex (1:2) and its stepwise association constants (K_1 and K_2) were evaluated to be log $K_1 = 1.6$ and log $K_2 = 4.1$, respectively. $\mathbf{1_R}$ also recognised $\mathbf{2_S}$ cooperatively and formed into a 1:3 complex in log $K_1 = 1.9$, log $K_2 = 1.2$ and log $K_3 = 3.8$. When we use racemic **2**, $\mathbf{1_R}$ exhibits unconventional enantioselectivity only towards $\mathbf{2_R}$ in a specific concentration region. It not only showed a chiral screening but also changed the stoichiometry depending on the guest chirality. These high enantioselectivity and stoichiometric modulation are effected by proper incorporation of the structural information of two enantiomers into the host and utilisation of multiple equilibrium characteristic of positive allosterism.

Keywords: host–guest chemistry; double-decker porphyrin; enantioselective recognition; allosteric effect

The design of synthetic allosteric systems is of great significance not only to regulate the complexation ability or the catalytic activity of receptors but also to attain high selectivity in a nonlinear fashion (*1*, *2*). Among them, the design of positive homotropic allosteric systems is the most attractive but most difficult one because the guest-binding information in a subunit should be passed to all other subunits in unison (*3*). The pivotal feature of positive homotropic allosterism is a nonlinear sigmoidal response to outside information, for example, the effector and/or substrate concentration, which then generates bistable OFF/ON states (*4*). It is expected, because of the multi-step cooperative binding mode, that the nonlinear sigmoidal response (binding isotherm) would generate high selectivity and specificity towards the effectors and/or substrates for the precise processing of molecular information in such allosteric systems.

We previously reported that a cerium(IV) bis(porphyrinato) double-decker complex, **DDPy8**, exhibits positive homotropic allosterism on binding cyclohexane-1R,2R-dicarboxylic acid ($\mathbf{2_R}$) through the hydrogen bonds to form the 1:4 **DDPy8**$\cdot(\mathbf{2_R})_4$ complex (Figure 1) (*4*). This is because the binding of the first $\mathbf{2_R}$ suppresses the rotation of two porphyrin rings to create three geometrically equivalent binding sites (*5*, *6*). When the structural information of $\mathbf{2_R}$ was input into such an allosteric host through a covalent bond, the conformation should be pre-organised complementary to $\mathbf{2_R}$. To confirm the hypothesis, we designed **DDPy7R** and demonstrated unconventional selectivity for $\mathbf{2_R}$ over $\mathbf{2_S}$ (Figure 1) (*7*). Herein, we designed a new host ($\mathbf{1_R}$), in which each porphyrin has one covalently bound $\mathbf{2_R}$ (Figure 1). Because of bridging two porphyrins by two intramolecular hydrogen bonds, one may expect the higher 'chiral memory effect' on the $\mathbf{2_R}$ vs. $\mathbf{2_S}$ selectivity. $\mathbf{1_R}$ was synthesised from Ce(IV) double-decker porphyrin of 5-(4-aminophenyl)-10,15,20-tripyridylporphyrin according to Scheme 1 and identified by ^{1}H NMR and MALDI-TOF-MS spectra (Figures S1 and S2 in Supplementary Material, available online).

Initially, we evaluated the conformation of $\mathbf{1_R}$ in the absence of guest in order to confirm the existence of intramolecular hydrogen bonding. The presence of intramolecular hydrogen bonds between the carboxylic acid groups and the pyridyl groups can be easily estimated from the rotational freedom of the two porphyrin rings. The shape of the circular dichroism (CD) signals observed for $\mathbf{1_R}$ was similar to that observed for **DDPy8**$\cdot(\mathbf{2_R})$ complex (*4*, *5*). As shown in Figure 2, $\mathbf{1_R}$ gave the positive CD around 310 nm, which was attributable to the chirality around the pyridyl groups (*5*). On the other hand, the CD signal around 310 nm disappeared by the addition of excess triethylamine (Figure 2). These observations are consistent with the intramolecular hydrogen bonding in $\mathbf{1_R}$ (*7*). The similarity in the CD spectral shape between $\mathbf{1_R}$ and **DDPy8**$\cdot(\mathbf{2_R})$ complex implies that $\mathbf{1_R}$ has been pre-organised so that it can readily accept $\mathbf{2_R}$ guest.

*Corresponding author. Email: takeuchi.masayuki@nims.go.jp

ISSN 1061-0278 print/ISSN 1029-0478 online

DOI: 10.1080/10610278.2010.510191
http://www.informaworld.com

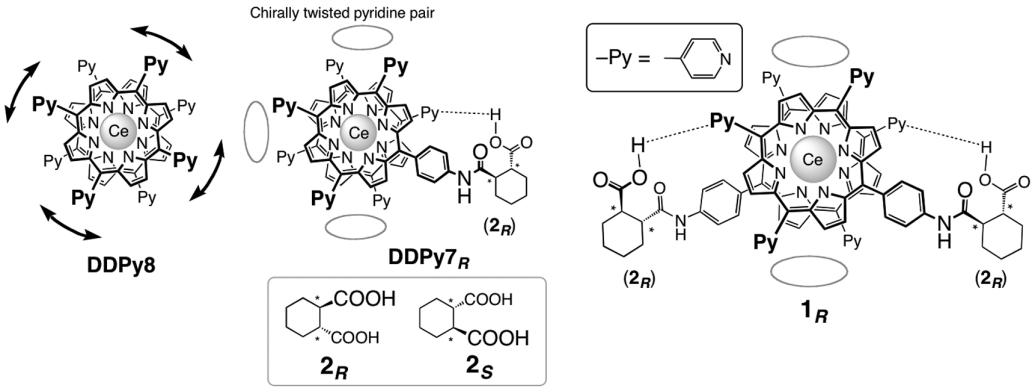

Figure 1. Chemical structures of hosts **DDPy8**, **DDPy7$_R$**, **1$_R$** and chiral guests **2**.

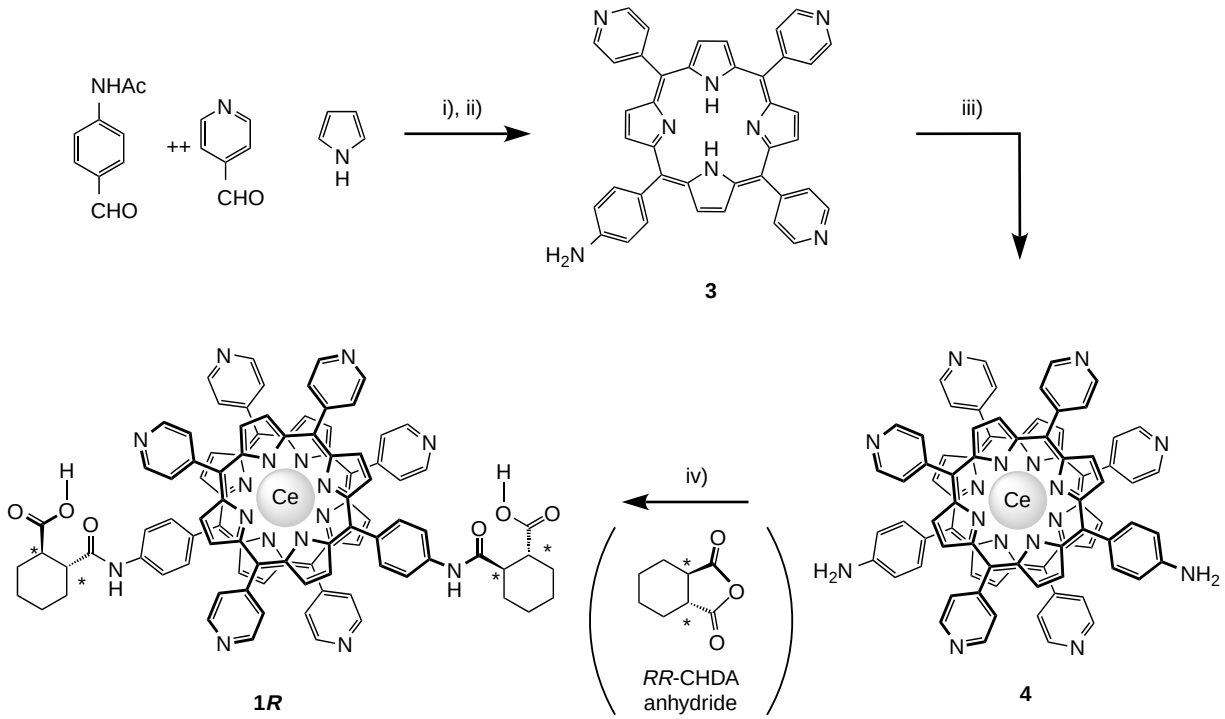

Scheme 1. *Reagent and conditions*: (i) propionic acid, reflux, 5 h; (ii) TFA water, reflux, 2 h (15% in total step); (iii) $Ce(acac)_3 \cdot 3H_2O$, *p-t*-BuPhNH$_2$, 1,2,4-trichlorobenzene, reflux, 6 h (24%) and (iv) **2$_R$** anhydride, dichloromethane, rt, 1 h (quant.).

The theoretical examination of the **1$_R$** structure also supports that the proposed structure is a reasonable one (vide infra).

We evaluated the formation of the **1$_R$**·**2** complexes in a tetrachloroethane (TCE)–tetrahydrofuran (THF) 30:1 (v/v) mixed solvent at 298 K using the CD spectral change induced upon the successive addition of **2** (Figure 3(a) and (b)). The CD intensity at 310 nm increased with the increase in the **2$_R$** concentration with tight isosbestic points, whereas it decreased with the increase in the **2$_S$** concentration. First, these guest-binding events were analysed using the Hill equation for plots of the CD intensity at 310 nm (Figure 3(c)) (*8*). From the slope of the linear Hill plots, we obtained Hill coefficient n_H values which were estimated to be 2.0 for the **1$_R$**·(**2$_R$**) complex and 2.8 for the **1$_R$**·(**2$_S$**) complex (Figure 3(d) and (e)). Generally, n_H is defined as the value related to a degree of cooperativity in a recognition process and the higher value of n_H (>1.0) means the higher degree of cooperativity. It is also known that the n_H value provides the information about the stoichiometry of the complex. The n_H value for **1$_R$**·(**2$_R$**) was 2.0, indicating that the complex consists of 1:2 host–guest ratio. To further corroborate this stoichiometry, we prepare the Job plot using the CD intensity at 310 nm. The peak appearing at $[\mathbf{1_R}]/([\mathbf{1_R}] + [\mathbf{2_R}]) = 0.33$ supports the view that the **1$_R$** host binds two guests cooperatively (Figure S3 in Supplementary Material, available online).

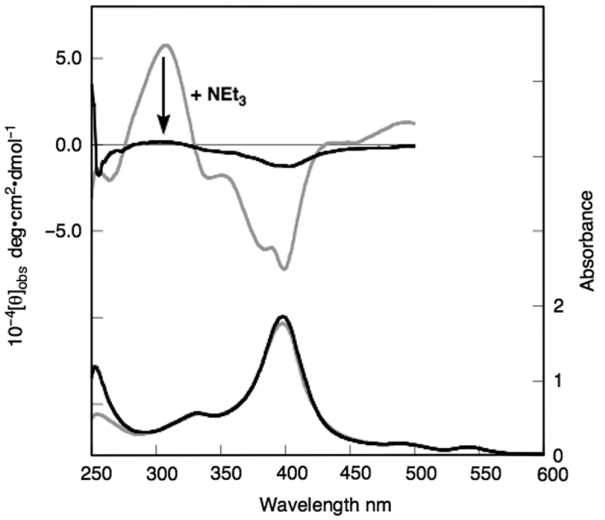

Figure 2. CD spectra of $\mathbf{1_R}$ (0.10 mmol dm^{-3}; light grey line) and $\mathbf{1_R}$ (0.10 mmol dm^{-3}) + triethylamine (100 mmol dm^{-3}; black line) in a TCE–THF 30:1 (v/v) mixed solvent at 298 K (cell length = 1.0 mm). The hydrogen bond-induced CD signal around 310 nm, which was assigned to the chiral pyridine pair, disappeared upon the addition of triethylamine.

We also analysed this binding isotherm according to the stepwise binding process and evaluated the association constants in detail by a nonlinear curve-fitting method assuming the stepwise association constants K_1 and K_2. They were estimated to be log $K_1 = 1.6$, log $K_2 = 4.1$ and log $K_{\text{total}} = 5.6$ (correlation coefficient, $R = 0.997$) for $\mathbf{2_R}$ (K_n/M^{-1}). The relation $K_1 < K_2$ clearly indicates that this guest-binding process features the positive homotropic allosterism. It may be a little curious that $\mathbf{1_R}$, being pre-organised suitably for the $\mathbf{2_R}$ binding, affords the sigmoidal curvature. We consider that $\mathbf{1_R}$ can still adopt several rotational conformers although the most stable one is that illustrated in Figure 4(a), bearing two intramolecular COOH—Py hydrogen bonds and two pairs of Py–Py guest-binding sites. The process where several conformers are optimised into the most stable one by the guest binding would be reflected by the sigmoidal curvature. On the other hand, the n_{H} value for the $\mathbf{1_R}\cdot(\mathbf{2_S})$ complex was estimated to be 2.8, indicating that the complex consists of 1:3 host–guest ratio, and the three binding sites are supplied for the $\mathbf{2_S}$ binding.[1] The stepwise analysis of the three binding steps provided log $K_1 = 1.9$, log $K_2 = 1.2$, log $K_3 = 3.8$ and log $K_{\text{total}} = 6.9$ (correlation coefficient, $R = 0.998$). The 1:3 molar ratio calls one possible host conformation to our mind that the intramolecular hydrogen bonds are formed between the pendent amide (CONH) groups, which eventually results in three pairs of Py–Py guest-binding sites suitable for $\mathbf{2_S}$ (Figure 4(c)).[2] The molecular modelling studies of $\mathbf{1_R}\cdot(\mathbf{2_R})_2$ complex and $\mathbf{1_R}\cdot(\mathbf{2_S})_3$ complex provided a few clues to rationalise the difference in the stoichiometry, depending on the guest chirality. In $\mathbf{1_R}\cdot(\mathbf{2_R})_2$, two intramolecular COOH—Py hydrogen bonds force the porphyrin rings to slightly twist leftward (from a top view). The orientation of two pairs of Py–Py binding sites thus generated is compatible with the orientation of two COOH groups in $\mathbf{2_R}$. In other words, the intramolecular hydrogen bonds used for porphyrin twisting can operate cooperatively with the intermolecular hydrogen bonds formed between $\mathbf{1_R}$ and $\mathbf{2_R}$. The resultant most stable complex has the 1:2 stoichiometry. In the $\mathbf{1_R}\cdot(\mathbf{2_S})_3$ complex, on the other hand, the leftward hydrogen bond orientation dominant in original $\mathbf{1_R}$ is opposite to the rightward hydrogen bond orientation in $\mathbf{2_S}$. Thus, the original intramolecular COOH—Py hydrogen bonds are collapsed to form one pendent amide–amide

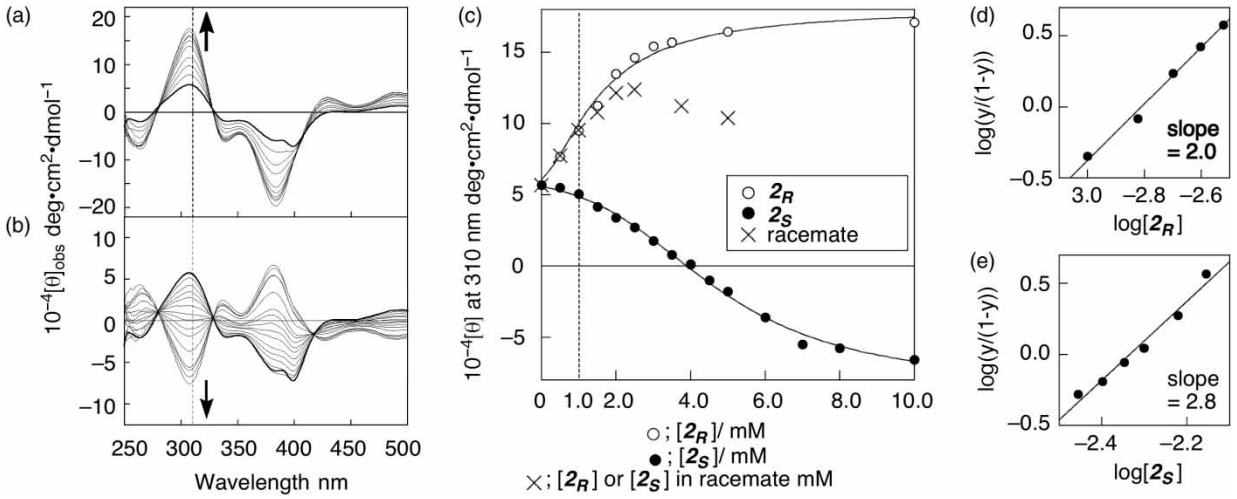

Figure 3. CD spectra of $\mathbf{1_R}$ (0.10 mmol dm^{-3}) recorded after the addition of (a) $\mathbf{2_R}$ and (b) $\mathbf{2_S}$ in a TCE–THF 30:1 (v/v) mixed solvent at 298 K (cell length = 1.0 mm). Bold lines in a and b are CD spectra of $\mathbf{1_R}$ in the absence of guest. (c) Plots of the CD intensity at 310 nm of $\mathbf{1_R}$ (0.10 mmol dm^{-3}) vs. concentration of **2** and the fitted theoretical curves (shown in solid lines) for 1:2 and 1:3 complexation with guest $\mathbf{2_R}$ and $\mathbf{2_S}$, respectively. Hill plots for the (d) $\mathbf{2_R}$ and (e) $\mathbf{2_S}$ recognition systems.

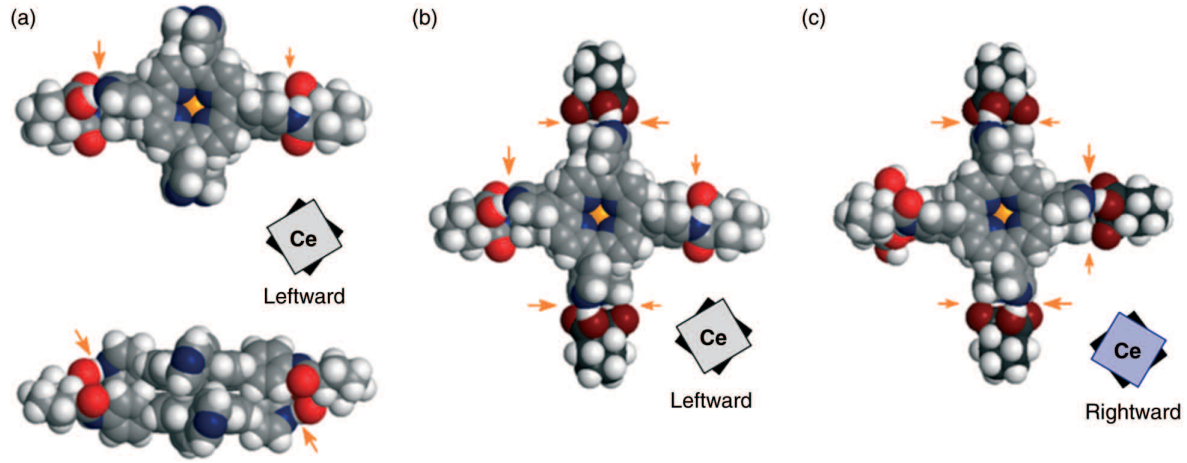

Figure 4. The energy minimised structures of (a) $\mathbf{1_R}$, (b) $\mathbf{1_R}\cdot(\mathbf{2_R})_2$ and (c) $\mathbf{1_R}\cdot(\mathbf{2_S})_3$ as generated by MM2 calculations with Insight II/Discover 3.0. Carbon and oxygen atoms of guest molecules are darkened for clarity. The arrows and symbols of stacked squares denote the hydrogen bonds and the twisting direction of two porphyrins. In the model for 1:3 $\mathbf{1_R}\cdot(\mathbf{2_S})_3$ complex, the intramolecular hydrogen bonds are collapsed.

linkage and three **2**-$(Py)_2$ linkages, all of which should have the rightward orientation.

To demonstrate the high enantioselectivity towards $\mathbf{2_R}$, we conducted the titration experiment using racemic **2**. Upon the addition of racemic **2**, the CD signal arising from the $\mathbf{1_R}\cdot(\mathbf{2_R})_2$ complex ($[\mathbf{1_R}] = 0.10\,\mathrm{mmol\,dm^{-3}}$) was the same as that of pure $\mathbf{2_R}$ (error is within 2%) until $[\mathbf{2_S}]$ in racemate reaches $1.0\,\mathrm{mmol\,dm^{-3}}$ and then gradually decreased because of the competitive formation of the $\mathbf{1_R}\cdot(\mathbf{2_S})_3$ complex (Figure 3(c) and S4). The critical $\mathbf{2_R}$ selectivity ($1.0\,\mathrm{mmol\,dm^{-3}}$) is higher than that observed for **DDPy7R** ($0.6\,\mathrm{mmol\,dm^{-3}}$) (*7*), supporting the improved chiral memory effect by two $\mathbf{2_R}$ groups covalently introduced into $\mathbf{1_R}$. Apparently, $\mathbf{1_R}$ exhibits unconventional enantioselectivity towards $\mathbf{2_R}$ in a specific concentration region, giving rise to the information that an error molecule ($\mathbf{2_S}$) is precisely filtered off by the control of the nonlinear responses (error filtering). This is affected by proper incorporation of the structural information of two enantiomers into the host and utilisation of multiple equilibrium characteristic of positive allosterism.

In conclusion, we consider that a new imprinting memory system can be designed by utilising the positive allosteric effect, and double-decker porphyrins act as excellent scaffolds for this kind of molecular design.

Experimental

General

All starting materials and solvents were purchased from Tokyo Kasei Chemicals (Chuo-ku, Tokyo, Japan) or Wako Chemicals (Osaka-shi, Osaka, Japan) and used as received. The ^{1}H NMR spectra were recorded on a Brucker DRX 600 (600 MHz) spectrometer. Chemical shifts are reported in ppm downfield from tetramethylsilane as the internal standard. Mass spectral data were obtained using a Perceptive Voyager RP MALDI-TOF mass spectrometer. CD spectra were recorded using JASCO J-720WI spectrophotometers.

Binding isotherm analysis

Cooperative guest-binding process was analysed according to the Hill equation: $\log[y/(1-y)] = n\log[\mathrm{guest}] + \log K$, where K, y and n_H are the association constant, the extent of complexation and the Hill coefficient, respectively. The slope and the intercept of the linear (Hill) plots allow K and n_H to be estimated; these values are useful measures of cooperativity. A higher value of n_H is related to a higher degree of cooperativity; the maximum value is equal to the number of binding sites. In the analysis of the binding isotherm from the Hill plot, we evaluated the concentration of the unbound guest – [guest] – by assuming that the 1:2, (vs. $\mathbf{2_R}$) or 1:3 (vs. $\mathbf{2_S}$) complex of $\mathbf{1_R}$ is formed quantitatively when the CD change is saturated. The stoichiometry of 1:2 (vs. $\mathbf{2_R}$) and 1:3 (vs. $\mathbf{2_S}$) was estimated by the continuous variation plot or the Hill plot. The stepwise binding constants were evaluated by the nonlinear least square curve-fitting based on the assumption of stoichiometry. The obtained theoretical curves are superimposed on Figure 3(c).

CD spectroscopy

A stock solution of **2** prepared in THF was added to a solution ($0.10\,\mathrm{mmol\,dm^{-3}}$) of $\mathbf{1_R}$ in 1,1,2,2-TCE. The solvent ratio of the measurement solution was TCE:THF = 30:1 (v/v). The CD spectra from 250 to 500 nm were recorded with a JASCO J-720WI spectropolarimeter at 10–15 different concentrations of guest

molecules. The measurement temperature was 278 K and the cell length was 1.0 mm.

Synthesis

Compound $\mathbf{1_R}$ was synthesised according to the procedures depicted in Scheme 1.

*Synthesis of porphyrin **3***

4-Acetamidobenzaldehyde (4.0 g, 24.5 mmol) and pyridine-4-carbaldehyde (2.5 g, 23.3 mmol) were dissolved in propionic acid (200 ml). After the mixture was stirred at 80°C for 30 min, pyrrole (3.4 ml, 50.0 mmol) was added. The solution was refluxed for 5 h. After cooling to room temperature (rt), ethylacetate (300 ml) was added to the flask and insoluble was removed by paper filtration. Half amount of solvent was removed *in vacuo* and *n*-hexene (500 ml) was added to the solution. A purple solid precipitate was collected by filtration. The purple solid was dissolved in mixed solvent of trifluoroacetic acid (30 ml) distilled water (30 ml) and the solution refluxed for 2 h. After cooling to rt, half amount of solvent was removed *in vacuo*, which was then neutralised with aqueous potassium carbonate solution until the colour of the solution changed from green to red. A crude product was extracted with dichloromethane from the aqueous phase. The organic extract was dried over anhydrous sodium sulphate and the solvents were removed. The resulting solid was purified by column chromatography (silica gel, dichloromethane/ethyl acetate/methanol = 5/5/1 (v/v/v)) to afford a purple solid (236 mg, 15% yield).

^{1}H NMR ($CDCl_3$, 600 MHz, *J*/Hz, rt); δ −2.84 (s, 2H, pyrrole-N*H*), 4.08 (br, 2H, NH_2), 7.09 (d, $J = 7.9$, 2H, Ph), 7.98 (d, $J = 7.9$, 2H, Ph), 8.16 (d, $J = 4.7$, 6H, Py), 8.81 (d, $J = 4.0$, 2H, pyrrole-C*H*), 8.84 (br-s, 4H, pyrrole-C*H*), 9.02 (d, $J = 4.1$, 2H, pyrrole-C*H*), 9.05 (d, $J = 5.0$, 6H, Py). MALDI-TOF mass [dithranol] *m*/*z* calc. for $[M]^+ = 632.24$, found 633.47.

*Synthesis of double-decker complex **4***

Mixture of porphyrin **3** (100 mg, 0.16 mmol), $Ce(acac)_3 \cdot 3H_2O$ (233 mg, 0.47 mmol) and *p*-*t*-butyl aniline (0.3 ml) in dry 1,2,4-trichlorobenzene (31 ml) was refluxed for 6 h under Ar. It was noted that the colour of the solution turned from red to green. After cooling to rt, the mixture was stirred for 15 min under air. Upon air oxidation of cerium, the colour of the solution turned to brown. The mixture was directly purified by column chromatography (silica gel, chloroform/methanol = 1/0–3/1 (v/v)) and gel column chromatography (Bio-Beads S-X3, chloroform) to afford a brown solid (26 mg, 24% yield). ^{1}H NMR ($CDCl_3$, 600 MHz, *J*/Hz, rt); δ 4.10 (br, 4H, NH_2), 6.2 (br, 2H, *exo*-*o*-Ph), 6.3 (br, 6H, *exo*-*o*-Py), 6.4 (br, 2H, *exo*-*m*-Ph), 7.5 (br, 2H, *endo*-*m*-Ph), 8.21–8.31 (m, 12H, pyrrole-C*H*), 8.45–8.51 (m, 4H, pyrrole-C*H*), 8.58 (br, 6H, *exo*-*m*-Py), 9.44 (br, 2H, *endo*-*o*-Ph) 9.5 (br, 12H, *endo*-*o*-Py, *endo*-*m*-Py). MALDI-TOF mass [dithranol] *m*/*z* calcd for $[M]^+ = 1400.36$, found 1400.73.

Synthesis of double-decker complex $\mathbf{1_R}$

Double-decker complex **3** (14.0 mg, 10.0 μmol) was dissolved in dichloromethane (3 ml). (1*R*,2*R*)-Cyclohexane-1,2-dicarboxylic anhydride (15.0 mg. 970 μmol) was added to this solution, which was then stirred at rt for 1 h. After the solvents were removed, the remaining solid was purified by gel column chromatography (Bio-Beads S-X3, chloroform). Precipitation treatment using dichloromethane ethyl acetate gave a brown solid (17 mg, quant.). ^{1}H NMR (pyridine-d_5, 600 MHz, *J*/Hz, −20°C); δ 1.18 (m, 2H, cyc-hex), 1.37 (m, 2H, cyc-hex), 1.65 (m, 2H, cyc-hex), 1.74 (m, 4H, cyc-hex), 1.96 (m, 2H, cyc-hex), 2.48 (m, 2H, cyc-hex), 2.57 (m, 2H, cyc-hex), 3.42 (m, 2H, cyc-hex), 3.62 (m, 2H, cyc-hex), 6.78-91 (m, 8H, *exo*-*o*-Ph and *exo*-*o*-Py), 8.15–8.35 (m, 2H, *exo*-*m*-Ph), 8.65–8.73 (m, 4H, pyrrole-C*H*), 8.77–8.82 (m, 16H, pyrrole-C*H*), 8.90–8.97 (m, 18H, *exo*-*m*-Py and CONH), 9.15–9.31 (m, 2H, *endo*-*m*-Ph), 9.61–9.67 (m, 6H, *endo*-*m*-Py), 9.93–10.0 (br, 8H, *endo*-*o*-Ph and *endo*-*o*-Py), 12.10 (m, 2H, COO*H*). MALDI-TOF mass [dithranol] *m*/*z* calcd for $[M]^+ = 1708.49$, found 1709.74.

Acknowledgements

T.I. thanks the JSPS Research Fellowship for Young Scientists for financial support. This study was supported partially by KAKENHI to M.T. from the Ministry of Education, Culture, Science, Sports and Technology, Japan.

Notes

1. Analysis of the stoichiometry for complex with $\mathbf{2_S}$ by continuous-variation plots did not indicate a significant change in the CD intensity because the concentration, $[\mathbf{1_R}] + [\mathbf{2_S}]$ was too low to form the complex as shown in Figure 3(c). Moreover, this concentration cannot be raised because of the precipitate formation
2. For the 1:3 $\mathbf{1_R} \cdot (\mathbf{2_S})_3$ complex, the COOH–COOH interaction between the remaining pendent substituents (see also Graphical abstract) would be possible; the theoretical estimation shown in Figure 4 indicates that the CONH–CONH interaction is more likely because of steric orientation of the hydrogen bonding sites. In other words, in the molecular modelling for $\mathbf{1_R} \cdot (\mathbf{2_S})_3$, formation of the amide dimer is sterically more favourable than the formation of carboxylic acid dimer

References

(1) (a) Kovbasyuk, L.; Krämer, R. *Chem. Rev.* **2004**, *104*, 3161–3188. (b) Takeuchi, M.; Ikeda, M.; Sugasaki, A.; Shinkai, S.

Acc. Chem. Res. **2001**, *34*, 865–873. (c) Nabeshima, T. *Coord. Chem. Rev.* **1996**, *148*, 151–169. (d) Rebek, J., Jr. *Acc. Chem. Res.* **1984**, *17*, 258–264.

(2) (a) Heo, J.; Mirkin, C.A. *Angew. Chem., Int. Ed.* **2006**, *45*, 941–944. (b) Botta, B.; Caporuscio, F.; Subissati, D.; Tafi, A.; Botta, M.; Filippi, A.; Speranza, M. *Angew. Chem., Int. Ed.* **2006**, *45*, 2717–2720. (c) Oliveri, C.G.; Gianneschi, N.C.; Nguyen, S.T.; Mirkin, C.A.; Stern, C.L.; Wawrzak, Z.; Pink, M. *J. Am. Chem. Soc.* **2006**, *128*, 16286–16296.

(3) (a) Setsune, J.; Watanabe, K. *J. Am. Chem. Soc.* **2008**, *130*, 2404–2405. (b) Sessler, J.L.; Tomat, E.; Lynch, V.M. *J. Am. Chem. Soc.* **2006**, *128*, 4184–4185. (c) Chang, K.-J.; Jang, H.-Y.; Jeong, K.-S. *Tetrahedron Lett.* **2006**, *47*, 4141–4144. (d) Kubo, Y.; Kitada,Y.; Wakabayashi, R.; Kishida, T.; Ayabe, M.; Kaneko, K.; Takeuchi, M.; Shinkai, S. *Angew. Chem., Int. Ed.* **2006**, *45*, 1548–1553.

(4) Takeuchi, M.; Imada, T.; Shinkai, S. *Angew. Chem., Int. Ed.* **1998**, *37*, 2096–2099.

(5) Ikeda, M.; Takeuchi, M.; Sugasaki, A.; Robertson, A.; Imada, T.; Shinkai, S. *Supramol. Chem.* **2000**, *12*, 321–338.

(6) Tashiro, K.; Konishi, K.; Aida, T. *Angew. Chem., Int. Ed. Engl.* **1997**, *36*, 856–858.

(7) Ikeda, T.; Hirata, O.; Takeuchi, M.; Shinkai, S. *J. Am. Chem. Soc.* **2006**, *128*, 16008–16009.

(8) Connors, K.A. *Binding Constants*; John Wiley and Sons: New York, 1987.